Template-Free Routes to Macroporous Monoliths of Nickel and Iron Oxides: Toward Porous Metals and Conformally Coated Pore Walls

Eric S. Toberer, Abhijeet Joshi, and Ram Seshadri*

Materials Department and Materials Research Laboratory, University of California, Santa Barbara, California 93106

Received October 14, 2004. Revised Manuscript Received February 1, 2005

In our continuing efforts to prepare macroporous monoliths of functional inorganic materials through novel template-free routes, we present here routes to porous NiO starting from Ni−Zn oxalates, and to porous $ZnFe_2O_4$ starting from Zn−Fe oxalates. Monolithic Ni has been prepared from porous NiO by hydrogen reduction, with retention of the macropore structure. Heating porous $ZnFe_2O_4$ under high hydrogen flow rates simultaneously reduces the metals and transports zinc in the vapor phase, leaving behind a macroporous Fe monolith. Robust monoliths with pore dimensions ranging from 1 to 5 μm have been formed in all cases, with narrow pore diameter distributions. To further functionalize the porous NiO monolith, we have dip-coated a lanthanum source and fired it in air to obtain a conformal coating of $La_4Ni_3O_{10}$ particles on the surfaces of the NiO pore walls. Unlike conventional dip-coating, the skeletal support is itself a reactant in this process, ensuring that the coating is well-dispersed on the pore walls.

Introduction

Our recent efforts in the area of macroporous inorganic materials have aimed at achieving the following goals: (i) To prepare monolithic macroporous inorganic materials without the use of any porous template, (ii) to make macroporous monoliths of increasingly complex, *functional* inorganic materials, and finally, (iii) to control porosity on a variety of length scales. The general philosophy that we have followed is to devise reactions in the solid state that lead to intimate mixtures of two insoluble phases with distinct chemical reactivity. Suitably leaching out one of the two phases obtains a macroporous monolith of the other. Intimately mixed two-phase systems have been obtained from single source precursors,[1] by rapid combustion synthesis,[2] and by metathesis reactions in the solid state.[3,4] None of these routes require preformed templates, and through some of them, complex functional materials such as magnetic or piezoelectric perovskite oxides have been obtained.[4]

Similar template-free approaches to macroporous materials have been devised, for example, by Gorte et al.[5] who have made composites of NiO and yttria-stabilized zirconia (YSZ), and then leached away the Ni after reduction to form porous YSZ. Suzuki et al. have used directionally solidified eutectic reactions followed by selective leaching to produce unidirectionally porous oxides.[6] They have also prepared porous $CaZrO_3$ by the reactive sintering of ZrO_2 with dolomite $CaMg(CO_3)_2$.[7]

The template-free routes described here can be considered as complementary to the now-traditional inverse-opal methods for obtaining macroporous inorganic materials with ordered pores.[8,9] It must be remarked that inverse-opal materials have become increasingly complex in their pore-wall chemistry, as exemplified by porous $LiNiO_2$,[10] porous hydroxyapatite,[11] and porous α-$LiAlO_2$.[12]

In this contribution, we demonstrate the formation of porous $Ni_{0.7}Zn_{0.3}O$ monoliths starting from a single-source Ni−Zn oxalate, $Ni_{0.5}Zn_{0.5}C_2O_4{\cdot}2H_2O$, by decomposing it to the oxides, followed by selective leaching of ZnO. Reduction of porous $Ni_{0.7}Zn_{0.3}O$ in 5% H_2/N_2 yields a Ni monolith with retention of the open pore structure. In a similar vein, decomposing the Fe−Zn oxalate $Fe_{0.5}Zn_{0.5}C_2O_4{\cdot}2H_2O$ gives an intimate mixture of spinel $ZnFe_2O_4$ and ZnO, from which removal of ZnO results in a porous $ZnFe_2O_4$ monolith. These sets of reactions show the versatility of oxalates, which are being used for this purpose for the first time; oxalates can be prepared from a number of mixed transition metals and are easily converted to oxides through calcination. Hydrogen reduction of the $ZnFe_2O_4$ spinel monolith has been carried out under conditions (rapid flow rates) which result in both the reduction of the oxide to elemental metals and the

* To whom correspondence should be addressed. E-mail: seshadri@mrl.ucsb.edu. Fax: (805) 893-8797.

(1) Rajamathi, M.; Thimmaiah, S.; Morgan, P.; Seshadri, R. *J. Mater. Chem.* **2001**, *11*, 2489.
(2) Panda, M.; Rajamathi, M.; Seshadri, R. *Chem. Mater.* **2002**, *14*, 4762.
(3) Panda, M.; Seshadri, R.; Gopalakrishnan, J. *Chem. Mater.* **2003**, *15*, 1554.
(4) Toberer, E. S.; Weaver, J. W.; Ramesha, K.; Seshadri, R. *Chem. Mater.* **2004**, *16*, 2194.
(5) Gorte, R.; Vohs, J. *J. Catal.* **2003**, *216*, 477.
(6) Suzuki, Y.; Yamada, T.; Sakakibara, S.; Ohji, T. *Ceram. Eng. Sci. Proc.* **2000**, *21*, 19.
(7) Suzuki, Y.; Morgan, P. E. D.; Ohji, T. *J. Am. Ceram. Soc.* **2000**, *83*, 2091.
(8) Holland, B.; Blanford, C.; Do, T.; Stein, A. *Chem. Mater.* **1999**, *11*, 795.
(9) Xia, Y.; Gates, B.; Yin, Y.; Lu, Y. *Adv. Mater.* **2000**, *12*, 693.
(10) Yan, H. W.; Sokolov, S.; Lytle, J. C.; Stein, A.; Zhang, F.; Smyrl, W. H. *J. Electrochem. Soc.* **2003**, *150*, A1102.
(11) Melde, B. J.; Stein, A. *Chem. Mater.* **2002**, *14*, 3326.
(12) Sokolov, S.; Bell, D.; Stein, A. *J. Am. Ceram. Soc.* **2003**, *86*, 1481.

10.1021/cm0401342 CCC: $30.25
Published on Web 03/17/2005

concurrent transport of Zn vapor. This reduction yields porous Fe monoliths in a single step. This is the first demonstration of such concurrent reduction and leaching of Zn from a mixed metal oxide.

We have additionally sought robust ways of *layering* functionality, i.e. coating the pore walls of simple macroporous materials with particles of more complex functional materials. To this end we demonstrate that a lanthanum source can be coated on the pore walls of macroporous nickel oxide. Upon firing, small crystals of of the $m = 3$ Ruddlesden−Popper phase[13] $La_4Ni_3O_{10}$ are formed evenly over the surface of the pore walls. We refer to such a coating technique in which the substrate is itself a reactant as "reactive conformal coating".

Experimental Section

Ni or Fe salts [$Ni(CH_3CO_2)_2 \cdot 4H_2O$ (19.91 g, 0.08 mol) or $FeCl_2 \cdot 4H_2O$ (15.90 g, 0.08 mol)] and $Zn(CH_3CO_2)_2 \cdot H_2O$ (30.26 g, 0.08 mol) were dissolved in 200 cm^3 of water and combined with 200 cm^3 of 1 M oxalic acid. The solution immediately became cloudy and the crystalline precipitate of $[M_{0.5}Zn_{0.5}(C_2O_4) \cdot 2H_2O$; M = Ni or Fe] was collected and repeatedly washed. The precipitated oxalate was dried and calcined as a powder at 873 K for 1 h. The resulting powder was ground by hand in an agate mortar and pestle, and then pressed into cylindrical pellets (13 mm diameter and approximately 1−2 mm high). Sintering of the oxides was achieved by firing the pellets in air at 1273 K for 12 h. To remove the second, ZnO phase, the pellets were placed in 250 cm^3 of 4 M NaOH at 337 K for 3 days, with the solution being replaced twice. Following the leaching, the pellets were washed in deionized water for a day with periodic replacement of the water and dried in an air oven at 353 K.

Porous metals were formed via the decomposition and selective leaching of the porous oxide described above. This was achieved by flowing 5% H_2/N_2 at 723−973 K for 3−12 h over the sample.

Pellets of porous NiO were placed in a solution of lanthanum acetate (10 g of lanthanum acetate in 20 cm^3 of dilute nitric acid), centrifuged, dried, and then fired in air at 1273 K. Following 5 dippings, the samples were heated at 1273 K for 1 h. A series of dippings that did not contain lanthanum but were otherwise identical were run as a control. The elemental composition of the coated material was examined with a JEOL 6300F scanning electron microscope equipped with an Oxford Inca X-ray system for energy-dispersive X-ray (EDX) analysis.

Powder X-ray diffraction (XRD) was recorded for all samples on a Scintag X2 diffractometer employing $\theta-2\theta$ geometry and Cu Kα radiation, operated at 45 kV and 35 mA, with a step size of 0.015 ° 2θ and step time of 4 s per step. Scanning electron microscopy (SEM) was performed using a FEI XL40 Sirion microscope. Samples for microscopy were prepared from the interior fracture surfaces of broken pellets. The samples were mounted on double-sided carbon tape and gold coated before imaging.

Results

The reactions explored in this work are summarized by the scheme shown in Figure 1. Aqueous solutions of oxalic acid and metal acetates react to precipitate a single-phase mixed-metal oxalate (a). A dense pellet was formed by firing the oxalate powder and pressing the resulting fine-grained oxide in a die (b). A dense two-phase monolith of MO/ZnO

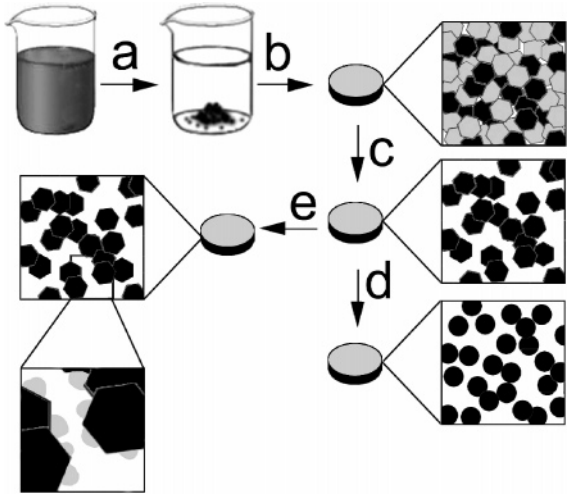

Figure 1. Scheme describing preparation of macroporous monoliths. A single-phase metal-organic precursor is formed in solution (a). The precipitated precursor is decomposed in air and the resulting powder is pressed into a pellet and sintered in air (b). The resulting oxide composite is leached in base to form a macroporous oxide (c). The oxide can be reduced in hydrogen to form a porous metal (d), or may be subjected to reactive dip coating (e).

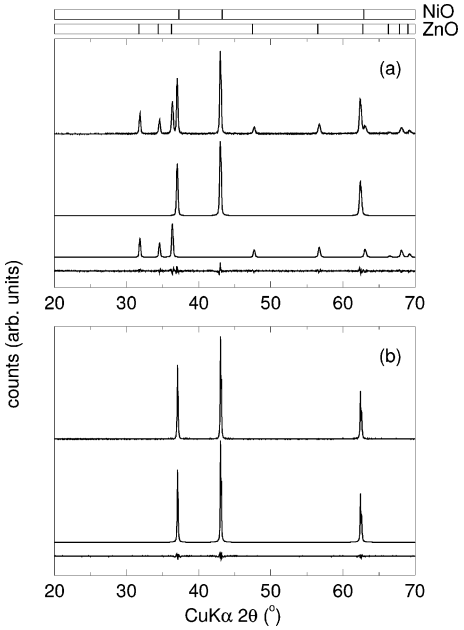

Figure 2. (a) Two-phase Rietveld fits of the monoliths formed by decomposition of Ni−Zn oxalate to the structures of ZnO and NiO. From top to bottom, the traces are data, fit to NiO, fit to ZnO, and difference profile. Expected peak positions for NiO and ZnO are indicated with vertical markers at the top. (b) Data, Rietveld fit, and difference profile of $Ni_{0.7}Zn_{0.3}O$ after leaching out ZnO with alkali.

(MO = $Ni_{0.7}Zn_{0.3}O$ or $ZnFe_2O_4$) was formed upon sintering the oxide pellet, and then rendered porous (c) by leaching ZnO in alkali. The resulting porous monolith could be reduced in hydrogen (d) and if required, leached again in alkali to form porous Ni or Fe monoliths. A conformal coat was formed along the inner surface of the NiO pore walls by dip-coating a new reactant followed by firing (e).

Formation of Porous Oxides. *$Ni_{0.7}Zn_{0.3}O$.* Figure 2 (a) shows the powder XRD pattern for the NiO/ZnO composite and Rietveld fit to the cubic $Fm\bar{3}m$ phase of NiO and hexagonal $P6_3mc$ phase of ZnO. The XND Rietveld code

(13) Ruddlesden, S. N.; Popper, P. *Acta Crystallogr.* **1958**, *11*, 54.

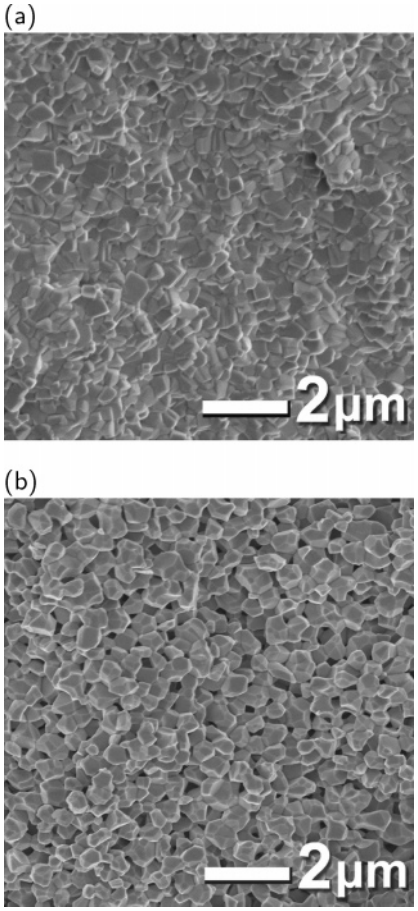

Figure 3. (a) SEM images of the fractured surface of $ZnO/Ni_{0.7}Zn_{0.3}O$ composite pellet formed from the decomposition of (Ni,Zn) oxalates. (b) SEM of the pellet after the ZnO phase is leached out with alkali, leaving behind porous $Ni_{0.7}Zn_{0.3}O$.

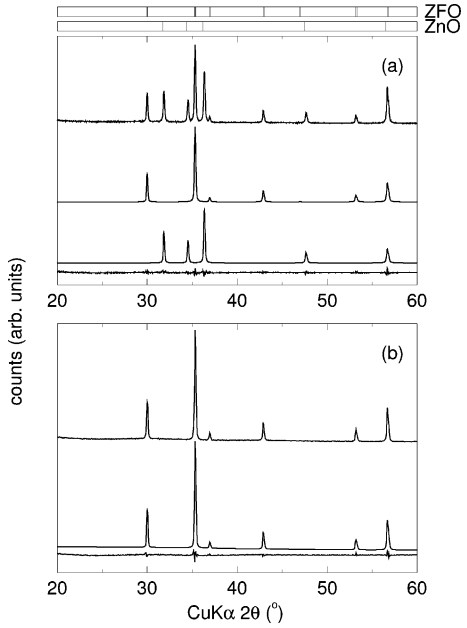

Figure 4. (a) Two-phase Rietveld fits of the monolith formed by decomposition of Zn−Fe oxalate to the structures of ZnO and $ZnFe_2O_4$. Expected peak positions for $ZnFe_2O_4$ (ZFO) and ZnO are indicated with vertical markers at the top. (b) Data, Rietveld fit, and difference profile of the $ZnFe_2O_4$ obtained after leaching out ZnO with alkali.

was employed for the refinements.[14] Rietveld scale factors give a NiO:ZnO mole ratio of 72:28 for a starting metal acetate ratio of 1:1. During the sintering process, there is no loss of mass, indicating that the starting metal ion ratio is preserved. The discrepancy (from 50:50) in the phase amounts of the two oxides ratio may be explained by substitution of Zn on the Ni site in rock-salt NiO. This is supported by the obtained NiO unit cell volume of 74.51 $Å^3$, which differs significantly from the reported value of 72.88 $Å^3$. Zinc substitution will increase the unit cell size, as the ionic radii of octahedral Ni^{2+} and Zn^{2+} are 0.69 and 0.74 Å, respectively. From the $Ni_{1-x}Zn_xO$:ZnO mole ratio, a value of $x = 0.3$ may be deduced. This value for the substitution onto the nickel site agrees with previous results employing other synthetic methods.[2]

Figure 2b shows the resulting powder XRD pattern and Rietveld fit for the washed monolith. Because the only phase present in the XRD pattern is NiO, it is clear that washing completely removes all hexagonal ZnO. No change in the $Ni_{1-x}Zn_xO$ cell parameters occurs during washing, indicating that the alkali leaching process selectively dissolves hexagonal ZnO and does not change the x value in the $Ni_{1-x}Zn_xO$. A 34% mass loss was observed, corresponding to an x value of 0.26 in $Ni_{1-x}Zn_xO$. This serves as an independent confirmation of substitution level. After leaching in base, the void volume fraction in the pellet was 55%, estimated from the mass and the physical dimensions. From the obtained mole ratios, the leaching of ZnO should give rise to a pellet density of 65%. This discrepancy could arise from incomplete densification during the sintering of the two-phase composite.

SEM images in Figure 3 show the cross sections of the NiO/ZnO composite sintered at 1273 K for 20 h (a) and the resulting washed pellet (b). The grains in the dense composite are 1−3 μm and there is almost no porosity. The coarsening of each phase appears to be greatly hindered by the presence of adjacent grains of the other phase, as the grain sizes for pellets sintered at 1273 K for 1 and 20 h are identical. The washed pellet in Figure 3b displays significant macroporosity, with a continuous network of pores that are 1−3 μm. The $Ni_{0.7}Zn_{0.3}O$ grains are well-faceted as they have not been reheated following the leaching process, and there is good connectivity between the grains.

$ZnFe_2O_4$. When the Zn/Fe oxalate was decomposed, pressed, and sintered, a two- phase composite of ZnO and $ZnFe_2O_4$ was obtained (Figure 4a). No other phase is observed in the X-ray pattern, and Rietveld refinement gives a ZnO:$ZnFe_2O_4$ mole ratio of 58:42. From the starting acetate ratio, we expect a 50:50 ratio. This discrepancy may be due to the different X-ray absorption cross sections of ZnO and the spinel. Following leaching in alkali solution, XRD analysis indicates that spinel $ZnFe_2O_4$ is the only phase present (Figure 4b).

The fracture surface of the ZnO:$ZnFe_2O_4$ composite reveals a dense monolith with 1−3 μm grains (Figure 5a). Following leaching of the ZnO phase, the pellet has a continuous network of 3 μm pores (Figure 5b). As the porosity is due to leaching in an external solution, the pores must be connected. The rather low pore volume fraction

(14) Bérar, J.; Garnier, P. *NIST Spec. Publ.* **1992**, *846*, 212.

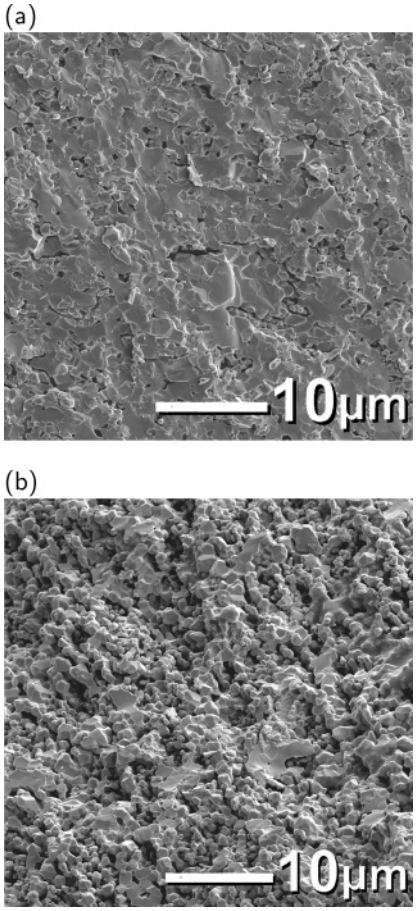

Figure 5. (a) SEM image of the sintered $ZnFe_2O_4$/ZnO composite in cross-section. (b) SEM image of porous $ZnFe_2O_4$ after leaching out ZnO in alkali.

indicated by the SEM image is to be expected from the composition; the leached species (ZnO) has only a third the number of cations as the species ($ZnFe_2O_4$) that is left behind.

Reduction to Porous Metal. *$Ni_{0.7}Zn_{0.3}$ to Ni*. Reduction of the porous $Ni_{0.7}Zn_{0.3}O$ pellet under 5% H_2/N_2 (typically between 723 and 973 K) yielded a strong monolith composed of Ni and ZnO. Rietveld refinement of the X-ray pattern combined with quantitative phase analysis gave Ni/ZnO mole ratio of 78:22 (Figure 6a). This mole ratio agrees with values obtained for the substitution of Zn into the NiO, as described above. The average Ni grain size was calculated to be 50 nm from Scherrer broadening. The remaining ZnO was leached out with alkali, leaving a porous Ni monolith as seen from XRD (Figure 6b).

The surface of the Ni pellet is shown in Figure 7. Pore diameters range from 0.5 to 1 μm and the pore walls are 1 μm in diameter. It is evident that the porosity of the starting oxide monolith is retained upon reduction. This is despite the significant mass transport of material which gives rise to increased necking and a quasi-continuous wall structure. Necking and rounding of the facets has occurred to such a degree that individual grains are difficult to observe. The structure of the porous metal monoliths obtained from these high-temperature reductions compares very favorably with the structure obtained in our previous work; in our prior attempts to make porous Ni monoliths, the pore structure arose from connected Ni crystals[1,2] and the pore walls were by no means quasi-continuous. As the mechanical strength

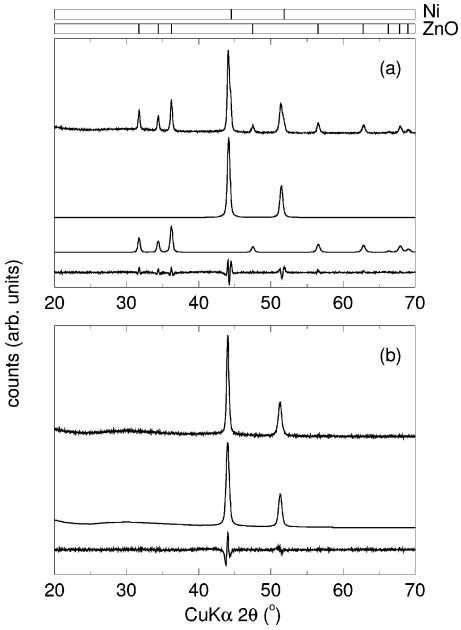

Figure 6. XRD pattern of products formed on reducing the $Ni_{0.7}Zn_{0.3}O$ in hydrogen. (a) Data, Rietveld fits to Ni and ZnO, and difference profile. (b) XRD data of the porous Ni after removal of ZnO in alkali, showing data, Rietveld fit to Ni, and the difference profile. Expected peak positions for Ni and ZnO are shown at the top.

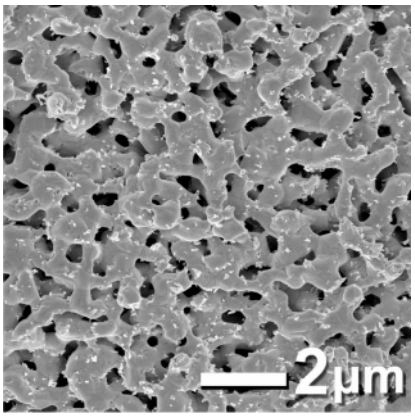

Figure 7. SEM image of the product obtained on reducing $Ni_{0.7}Zn_{0.3}O$ in hydrogen. The continuous network is Ni metal, and the small white specks are ZnO.

of porous materials depends heavily on the extent of necking, the morphologies obtained here are desirable.

$ZnFe_2O_4$ to Fe. Similarly, reduction of porous $ZnFe_2O_4$ in 5% H_2 at 723 K produced ZnO and Fe. Firing for 12 h in hydrogen induces a 20% mass loss, which agrees with the complete conversion of $ZnFe_2O_4$ to ZnO and Fe. From the XRD profile, ZnO and Fe are the only phases present. Rietveld refinement of the reduced monolith reveals a ZnO/Fe ratio of 36:64, in agreement with our understanding of the decomposition. Leaching in alkali yields phase pure Fe with a 48% mass loss corresponding to the dissolution of ZnO.

When porous $ZnFe_2O_4$ was reduced at a higher temperature of 973 K for 12 h with relatively high gas flow rates, the XRD pattern showed no other phase than Fe. The total mass loss was 67% which agrees with expected weight loss (65%) for the conversion of a 1:1 ratio of ZnO/$ZnFe_2O_4$ to pure Fe with loss of all Zn and ZnO. At such an elevated temperature in a hydrogen atmosphere, ZnO is reduced to elemental Zn

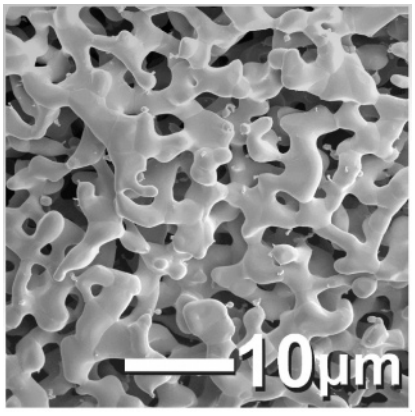

Figure 8. SEM image of porous Fe obtained from porous $ZnFe_2O_4$ by reduction in hydrogen and vapor-phase leaching of ZnO.

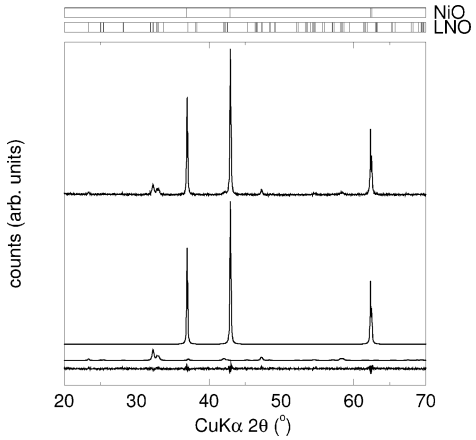

Figure 9. XRD pattern and Rietveld fit of $Ni_{0.7}Zn_{0.3}O$ with a conformal coating of $La_4Ni_3O_{10}$ (LNO). Data, fits to the different phases, and the difference profile are displayed, along with vertical lines showing expected peak positions.

(mp 692.5 K[15]). The mass loss is due to the vapor phase transport of the Zn out of the hot zone of the furnace. This is supported by the observation of Zn whiskers depositing at colder parts of the tube furnace. SEM imaging of the cross-section shows a porous monolith with a morphology similar to that of the porous nickel (Figure 8). Pore diameters and pore walls range from 1 to 5 μm. The porous monolith is quite robust and shows a high degree of necking.

Conformal Coating of the Porous NiO Monoliths. For conformal coating, the porous $Ni_{0.7}Zn_{0.3}O$ monolith was repeatedly dipped in saturated lanthanum acetate solution followed by firing at 1273 K for 1 h. The Rietveld fit to the XRD powder diffraction data (Figure 9) shows two phases: $Ni_{0.7}Zn_{0.3}O$ and the Ruddlesden−Popper phase $La_4Ni_3O_{10}$.[16] From the Scherrer broadening, the average $La_4Ni_3O_{10}$ grain size is 40 nm. Quantitative phase analysis gives a NiO/$La_4Ni_3O_{10}$ mole ratio of 90:10. SEM imaging of the inner fracture surface of the pellet reveals a coating of submicron particles (30−400 nm) along the surface of the porous $Ni_{0.7}Zn_{0.3}O$ (Figure 10). SEM imaging of the control sample (dipping without La) did not show any evidence of these submicron particles. On the basis of the agreement between

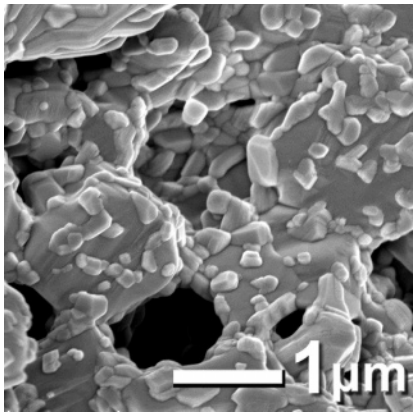

Figure 10. SEM image of conformal coating of $La_4Ni_3O_{10}$ submicron particles on inner surface of porous $Ni_{0.7}Zn_{0.3}O$.

the SEM analysis and XRD line broadening, we believe $La_4Ni_3O_{10}$ forms a conformal coating of submicron particles along the inner surface of the $Ni_{0.7}Zn_{0.3}O$. As the dipping process is additive, it is possible to adjust the coverage of the conformal coating by changing the solution concentration or number of dipping cycles.

Discussion

Selective leaching of one phase from a two-phase composite has proved to be a powerful method for forming porous, functional inorganic materials. In this work, we have demonstrated that mixed metal oxalate precursors are very useful starting materials for the preparation of such two-phase composites, and porous rock-salt and spinel oxides can be produced starting from oxalates, using successive decomposition and leaching steps. In our prior work on the preparation of macroporous monoliths,[1−4] we made use of temperature as the independent thermodynamic variable to induce phase segregation between inorganic species, accompanied by, or as a consequence of chemical change. In this work, we emphasize that oxygen partial pressure (through reducing atmospheres) can also be used as an independent variable in inducing phase segregation of one phase into two immiscible phases. Hydrogen reduction converts $Ni_{0.7}Zn_{0.3}O$ to Ni and ZnO, and $ZnFe_2O_4$ to Fe and ZnO. ZnO is a sacrificial phase which can be leached to leave behind a porous monolith of Ni or Fe.

We emphasize here that macroporous materials are not high surface area materials. A simple model for the monoliths reported here is to think of them as a collection of cubes, typically about 1.5 μm on edge. If these cubes have a density of approximately 7000 kg m^{-3}, then even if all the cubes were completely separated, the total surface area would less than 0.5 m^2g^{-1}. This is not a regime of surface area that could be probed by BET measurements with any accuracy. Clearly, to increase the surface area of macroporous materials, the walls of the materials need to be rendered porous on a finer scale. In fact, such hierarchically porous materials are current under investigation.

We have additionally demonstrated in this work that functionality can be *layered* on to the walls of porous monoliths. For this, we have used a process of reactive dip-coating where the pore walls themselves serve as a reac-

(15) Lide, D. R. *CRC Handbook of Chemistry and Physics*, 80th ed.; CRC Press: Boca Raton, FL, 2000.
(16) Zhang, Z.; Greenblatt, M. *J. Solid State Chem.* **1995**, *117*, 236.

tant: $La_4Ni_3O_{10}$ was formed as a conformal coating on the pore walls of macroporous $Ni_{0.7}Zn_{0.3}O$. It is interesting that this particular phase, the $m = 3$ Ruddlesden−Popper phase, is formed, rather than the simpler perovskite, $LaNiO_3$ ($m = \infty$) or the $m = 1$ La_2NiO_4 phase, or even $m = 2$ $La_3Ni_2O_7$. The formation of the $m = 3$ phase is perhaps related to Ni attaining an appropriate oxidation state, less than Ni(III) which would be required by $LaNiO_3$. The formation is in agreement with the known $La_2O_3-NiO-{}^1/_2O_2$ phase behavior.[17] We note that such reactive conformal coating provides numerous possibilities for controlling triple point boundaries formed between two inorganic phases, and a third reactive vapor phase. Triple point boundaries are believed to play a crucial role in oxide fuel cells.[18]

Acknowledgment. We gratefully acknowledge the contributions of Lily Lee to the initial stages of this work. E.S.T. is supported by an IGERT fellowship from the NSF (award DGE-9987618). A.J. acknowledges the California NanoSystems Institute for an INSET internship, supported by the NSF through the REU program (award EEC-0139138). This work was supported by the UCSB Academic Senate through a Research Grant, and made use of facilities of the Materials Research Laboratory supported by the NSF (award DMR00-80034).

CM0401342

(17) Petrov, A. N.; Cherepanov, V. A.; Zuyev, A. Y.; Zhukovsky, V. M. *J. Solid State Chem.* **1988**, *77*, 1.

(18) Haile, S. *Acta Mater.* **2003**, *51*, 5981.